

The Electronic Structure and Spectrum of  $\text{Mo}(\text{CN})_8^{3-}$ 

M. F. A. Hendrickx,\* L. F. Chibotaru, and A. Ceulemans

Department of Chemistry, University of Leuven, Celestijnenlaan 200F, B-3001 Leuven, Belgium

Received July 14, 2002

State of the art CASSCF and CASPT2 calculations have been performed to elucidate the nature of the electronic transitions observed in the experimental spectrum of the octacyanomolybdate(V) cation. Assuming a triangular dodecahedral structure for this complex gives a convincing agreement between theory and experiment. All absorption bands are assigned to low-lying charge-transfer transitions involving excitations from ligand orbitals to  $4d_{x^2-y^2}$ . The calculated molecular orbitals reveal weak  $\pi$  interactions between the metal and ligand orbitals, compared to much stronger  $\sigma$  interactions. This calculated electronic structure substantiates the previous hypothesis concerning the giant spin ground states of magnetic clusters and networks containing  $\text{Mo}(\text{CN})_8^{3-}$  as a constituent part.

## Introduction

Cyanide complexes of transition metal ions are important building blocks of magnetic clusters and networks.<sup>1</sup> Typical examples are the cyano-bridged perovskites of the Prussian blue family. In these complexes the core consists of a hexacyanometalate. Strong magnetic interactions through the cyanide bridge between C- and N-coordinated metal ions,  $\text{M}_1\text{—CN—M}_2$ , explain the use of these complexes in high- $T_c$  molecular-based magnets.<sup>2</sup> Recently novel cyano-based clusters have been reported, having octacyanometalates  $\text{Mo}(\text{CN})_8^{3-}$  and  $\text{W}(\text{CN})_8^{3-}$  as building blocks.<sup>3,4</sup> Examples are the  $\text{Mn}_9\text{Mo}_6$  and  $\text{Mn}_9\text{W}_9$  fully capped cubane clusters which exhibit giant spin ground states. For an understanding of the origin of the observed ferromagnetism a hypothesis

based on the covalent interactions between the metal cation and the cyanide ligands has been put forward.<sup>5</sup> Surprisingly, the electronic structure of the key octacyano complexes in these clusters is almost entirely unknown, and the 1963 paper of Perumareddi et al.<sup>6</sup> still is the primary source for spectral information.

To fill this gap we initiate in this paper a detailed study of the electronic structure of  $\text{Mo}(\text{CN})_8^{3-}$ . The synthesis of the octacyanomolybdate(V) complex was first reported by Bucknall and Wardlaw back in 1927.<sup>7</sup> Since then there has been a debate in the literature concerning its geometrical structure as well as on the nature of the electronic transitions responsible for the observed absorption bands. For eight coordinated complexes in general two conformations stand out, a dodecahedral structure possessing a  $D_{2d}$  symmetry and a tetragonal antiprism of  $D_{4d}$  symmetry. For the  $d^1$  complex  $\text{Mo}(\text{CN})_8^{3-}$  and the analogous  $\text{W}(\text{CN})_8^{3-}$  complex the experimental evidence points to the existence of both structures, the actual geometry of the complex being determined by the nature of its surrounding. The spectrum of  $\text{Mo}(\text{CN})_8^{3-}$  in aqueous solution was first published and assigned by Perumareddi et al. in 1963. On the basis of ligand field calculations the intense absorption bands were attributed to transitions among the 4d orbitals, which were considered to be split by a dodecahedral ligand field. This assignment was later contested by Golebiewski et al.,<sup>8</sup> who performed an elementary electronic structure SCCC MO (self-consistency

\* To whom correspondence should be addressed. E-mail: marc.hendrickx@chem.kuleuven.ac.be.

- (1) (a) Mallah, T.; Auburger, C.; Verdaguer, M.; Veillet, P. *J. Chem. Soc., Chem. Commun.* **1995**, 61. (b) El Fallah, S. M.; Rentschler, E.; Caneschi, A.; Sessoli, R.; Gatteschi, D. *Angew. Chem.* **1996**, *108*, 2081–2083; *Angew. Chem., Int. Ed. Engl.* **1996**, *35*, 1947. (c) Scullier, A.; Mallah, T.; Verdaguer, M.; Nivorozhkin, A.; Tholence, J.-L.; Veillet, P. *New J. Chem.* **1996**, *20*, 1. (d) Heinrich, J. L.; Berseth, P. A.; Long, J. R. *Chem. Commun.* **1998**, 1231. (e) Ferlay, S.; Mallah, T.; Quahès, R.; Veillet, P.; Verdaguer, M. *Inorg. Chem.* **1999**, *38*, 229. (f) Mallah, T.; Marvilliers, A.; Rivière, E. *Philos. Trans. R. Soc. Ser. A* **1999**, *357*, 3139.
- (2) (a) Griebler, W.-D.; Babel, D. Z. *Naturforsch. B* **1982**, *37*, 832. (b) Gadet, V.; Mallah, T.; Castro, I.; Verdaguer, M.; Veillet, P. *J. Am. Chem. Soc.* **1992**, *114*, 9213. (c) Mallah, T.; Thiebaut, S.; Verdaguer, M.; Veillet, P. *Science* **1993**, *262*, 1554–1557. (d) Ferlay, S.; Mallah, T.; Quahès, R.; Veillet, P.; Verdaguer, M. *Nature* **1995**, *378*, 701. (e) Holmes, S. M.; Girolami, G. S. *J. Am. Chem. Soc.* **1999**, *121*, 5593.
- (3) Larionova, J.; Gross, M.; Pilkington, M.; Andres, H.; Stoeckli-Evans, S.; Güdel, H. U.; Decurtins, S. *Angew. Chem.* **2000**, *112*, 1579–1583; *Angew. Chem., Int. Ed.* **2000**, *39*, 1605–1609.
- (4) Zhong, Z. J.; Seino, H.; Mizobe, Y.; Hidai, M.; Fijishima, A.; Ohkoshi, S.-I.; Hashimoto, K. *J. Am. Chem. Soc.* **2000**, *122*, 2952.

(5) Chibotaru, L. F.; Mironov, V. S.; Ceulemans, A. *Angew. Chem., Int. Ed.* **2001**, *40*, 4429.

(6) Perumareddi, J. R.; Liehr, A. D.; Adamson, A. W. *J. Am. Chem. Soc.* **1963**, *85*, 249.

(7) Bucknall, W. R.; Wardlaw, W. J. *Chem. Soc.* **1927**, 2986.

(8) Golebiewski, A.; Kowalski, H. *Theor. Chim. Acta* **1968**, *12*, 293.

with respect to charges and configurations) calculation based on a square-antiprismatic arrangement of the ligands around the molybdenum(V) cation. According to their findings all the observed bands in the electronic spectrum are due to charge-transfer transitions involving excitations from the ligand orbitals to the lowest lying 4d orbital of the metal ion. The authors reached this conclusion after assuming that the symmetry-allowed charge-transfer transitions are 10 times more intense than the symmetry-forbidden ones and 100 times more intense than the d–d transitions. No attempt was made to calculate oscillator strengths.

### Computational Method

In giant spin clusters the geometry of  $\text{Mo}(\text{CN})_8^{3-}$  is found to be nearly a trigonal dodecahedron.<sup>3</sup> In order to exploit the advantages of symmetry we carried out calculations for an idealized dodecahedron in which all the carbon atoms and all the nitrogen atoms are equidistant from the central metal cation. The Mo–C and C–N distances were set at their experimental value of 2.14 and 1.14 Å,<sup>9</sup> respectively, with linear Mo–C–N bonds. The origin of the coordinate system used in the calculations is placed in the molybdenum cation. The z axis coincides with the  $S_4$  axis of the  $D_{2d}$  point group while the x and y axes are situated on the two  $C_2$  axes. Besides the results for the isolated  $\text{Mo}(\text{CN})_8^{3-}$  anion a second series of calculations were carried out in which the effect of the complete crystal surroundings is incorporated by means of a limited set of counterions, the charge of each of these ions being determined by a fit of the Madelung potential<sup>10</sup> in the region of  $\text{Mo}(\text{CN})_8^{3-}$ . Incorporating the counterions lowers the symmetry to  $D_2$ .

For the carbon and nitrogen atom a basis set of the general contraction type was selected. Extended experience has shown that an atomic natural orbital (ANO) set based on a rather small number of primitive Gaussian type functions is sufficient to give a good description of the electronic spectra of transition metal complexes.<sup>11</sup> For both these atoms three s-type orbitals, two p-type orbitals, and one d-type orbital of the ANO-S<sup>12</sup> basis as implemented in the MOLCAS.5.0 suite of programs were chosen. For the molybdenum cation two effective core potentials (ECP) which incorporate relativistic effects and the corresponding basis set were employed. The first one consisted of the ECP basis set of Hay and Wadt<sup>13</sup> widely known as LANL2DZ (contraction: [3s, 3p, 2d]), the second one being a [3s, 3p, 4d] basis set as constructed by Barandiaran et al.<sup>14</sup> In combination with the ANO basis sets of carbon and nitrogen all relevant transitions were calculated twice, once with the Hay and Wadt basis and once with the Barandiaran basis. Comparison of two sets of transition energies showed an average deviation of about 500  $\text{cm}^{-1}$ , the difference never exceeding 1100  $\text{cm}^{-1}$ . Both basis sets are therefore equally suitable for the study of the electronic structure of  $\text{Mo}(\text{CN})_8^{3-}$ , both leading to the same conclusions. For the presentation of the computational results and their interpretation in the following sections we have used arbitrarily the data obtained

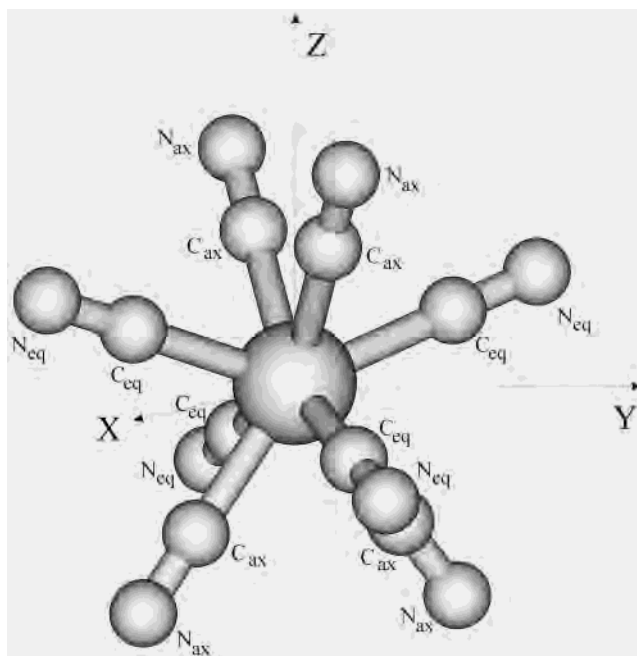


**Figure 1.** Idealized dodecahedral structure of  $\text{Mo}(\text{CN})_8^{3-}$  and coordinate system as used in the calculations.

by the Barandiaran basis. From this discussion of the electronic structure it will become clear that a multireference approach for the calculation of the various states is a necessity. Hence, the computational method of choice is obviously CASSCF to account for the near-degeneracy effects, followed by second-order perturbation (CASPT2) calculations for the incorporation of a sufficient amount of dynamic correlation. In the latter method all electrons are correlated with the exception of the 1s electrons of carbon and nitrogen, and of course the core of the molybdenum (ECP basis). The total number of electrons correlated at the CAPSPT2 level amounts to 87 for the Barandiaran basis and 89 for the Hay and Wadt basis. The MOLCAS.5.0 software<sup>15</sup> was used throughout. All calculations were carried out within the  $D_2$  point group, and therefore in discussing the results the irreducible representations (irreps) of this point group will be used. However, deviations from  $D_{2d}$  are always very small and when more appropriate the orbitals and states are classified according to  $D_{2d}$ . In this case it will be indicated explicitly in the text. For the sake of completeness we have included in a last section results obtained for the square-antiprism isomer of  $\text{Mo}(\text{CN})_8^{3-}$ . In this way our conclusions regarding the experimental spectrum can be substantiated.

### Results and Discussion

The free cyanide ion is known to bind to the transition metal cations by means of the  $1\pi$ ,  $2\pi^*$ , and  $5\sigma$  orbitals. Within the dodecahedral  $(\text{CN})_8^{8-}$  cluster there are two sets of symmetry equivalent cyanide ligands. A first set of four ligands is situated close to the  $S_4$  principal axis (z axis) and is denoted in Figure 1 by the subscript ax (abbreviation for axial), whereas the second set of four ligands is closer to

- (9) Corden, B. J.; Cunningham, J. A.; Eisenberg, R. *Inorg. Chem.* **1970**, 9, 356.  
 (10) Almlöf, J.; Wahlgren, U. *Theor. Chim. Acta* **1973**, 28, 161.  
 (11) Pierloot, K.; Van Praet, E.; Vanquickenborne, L. G. *J. Phys. Chem.* **1993**, 97, 12220.  
 (12) Pierloot, K.; Dumez, B.; Widmark, P.-O.; Roos, B. O. *Theor. Chim. Acta* **1995**, 90, 87.  
 (13) Hay, P. J.; Wadt, W. R. *J. Chem. Phys.* **1985**, 82, 270. Hay, P. J.; Wadt, W. R. *J. Chem. Phys.* **1985**, 82, 284; Hay, P. J.; Wadt, W. R. *J. Chem. Phys.* **1985**, 82, 299.  
 (14) Barandiaran, Z.; Seijo, L.; Huzinaga, S. *J. Chem. Phys.* **1990**, 93, 5843.

- (15) Andersson, K.; Barysz, M.; Bernhardsson, A.; Blomberg, M. R. A.; Carissan, Y.; Cooper, D. L.; Cossi, M.; Fleig, T.; Fülcher, M. P.; Gagliardi, L.; de Graaf, C.; Hess, B. A.; Karlström, G.; Lindh, R.; Malmqvist, P.-Å.; Neogrády, P.; Olsen, J.; Roos, B. O.; Schimmelpfennig, B.; Schütz, M.; Seijo, L.; Serrano-Andrés, L.; Siegbahn, P. E. M.; Ståhring, J.; Thorsteinsson, T.; Veryazov, V.; Wierzbowska, M.; Widmark, P.-O. *MOLCAS*, version 5.0; Lund University: Lund, Sweden 2001.

the equatorial plane ( $xy$  plane) and is denoted as eq in Figure 1. The orbitals for both sets give rise to the same number of irreps of the  $D_{2d}$  point group:  $a_1$ ,  $b_2$ , and  $e$  for the  $\sigma$  orbitals and  $a_1$ ,  $a_2$ ,  $b_1$ ,  $b_2$ , and  $2e$  for the  $1\pi$  and  $2\pi^*$  orbitals. Since both sets of cyanides are equidistant from the central metal cation and since there is no direct bonding between neighboring ligands, the splitting of the various levels is small. Taking further into account that the  $\pi$  and the  $5\sigma$  orbitals are close energetically to each other in complexes,<sup>16</sup> strong near-degeneracy effects can be expected. Incorporating point charges at the crystal positions of the counterions lowers the symmetry to  $D_2$ , thereby splitting the  $e$  irrep in  $b_2$  and  $b_3$ , while  $a_1$ ,  $b_1$  and  $a_2$ ,  $b_2$  subduce to  $a$  and  $b_1$ , respectively.

For the purpose of understanding the electronic structure of  $\text{Mo}(\text{CN})_8^{3-}$  preliminary CASSCF calculations were carried using an active space made up of, besides the five  $d$  orbitals of the metal, an occupied  $\sigma$  or  $\pi$  orbital (depending on the results of the calculation) and one unoccupied  $\pi^*$  orbital per irreducible representation of  $D_2$ . The resulting active space can be described as distributing 9 electrons among 13 orbitals (9i13). The three lowest roots of  $^2A$  symmetry and the two lowest roots of  $^2B_1$  and  $^2B_2$  symmetry were calculated. From these results it could be concluded that the ground state of the complex corresponds to a  $^2A$  ( $^2B_1$  in  $D_{2d}$ ) in which the unpaired electron occupies the  $d_{x^2-y^2}$  orbital. The most remarkable result is that the lowest lying excited states are of the charge-transfer type and more in particular of the type where an electron is transferred from a ligand orbital to the metal  $d_{x^2-y^2}$  (CTLM). The highest  $^2A$  and  $^2B_1$  states correspond to transitions from the highest ligand orbitals to  $d_z^2$ , the excitation energies amounting to more than  $50000\text{ cm}^{-1}$ . An analysis of the CASSCF wave function revealed that the  $2\pi^*$  orbitals contribute much less to all of the wave functions than the  $1\pi$  and  $5\sigma$  orbitals and explains the finding that there are no low-lying  $d_{x^2-y^2} \rightarrow 2\pi^*$  (CTML) transitions. The picture emerging from these results places the  $d_{x^2-y^2}$  orbital well below  $d_z^2$ , both situated between the low-lying occupied ( $5\sigma$ ,  $1\pi$ ) levels and the high-lying  $2\pi^*$  levels, however much closer to the occupied ligand orbitals. The high formal oxidation state of the molybdenum cation and large energy gap between the HOMO and the LUMO of the free cyanide anion are consistent with this description of the electronic structure of the dodecahedral  $\text{Mo}(\text{CN})_8^{3-}$ .

From the large number of ( $5\sigma$ ,  $1\pi$ ) levels and the expected small splitting one must anticipate that more CTLM transitions need to be considered. To achieve this the  $2\pi^*$  orbitals in the active space were replaced in each of the four irreps by an additional occupied ligand orbital. This resulted in CASSCF calculations in which 17 electrons are distributed among 13 orbitals (17i13). This is the largest active space for which the active orbitals are spread out evenly over the different irreps, which is still computable and for which each state considered is described by the same active space. The calculated CASPT2 excitation energies are collected in the lower part of Table 1. They confirm the ideas about the

**Table 1.** Explorative Calculations of the Electronic Structure of  $\text{Mo}(\text{CN})_6^{3-}$ <sup>a</sup>

active space	excited state	excitation energy ( $\text{cm}^{-1}$ )	nature of transition
9i13	$^2A$	29888	62% CTLM ( $14a \rightarrow x^2-y^2$ ), 30% LF ( $x^2-y^2 \rightarrow z^2$ )
	$^2A$	31848	30% CTLM ( $14a \rightarrow x^2-y^2$ ), 63% LF ( $x^2-y^2 \rightarrow z^2$ )
	$^2A$	50154	86% CTLM ( $14a \rightarrow z^2$ )
	$^2B_1$	36518	90% CTLM ( $15b \rightarrow x^2-y^2$ )
	$^2B_1$	52587	96% CTLM ( $15b_1 \rightarrow z^2$ )
	$^2B_2$	28904	84% CTLM ( $15b_2 \rightarrow x^2-y^2$ )
17i13	$^2A$	44845	90% LF ( $x^2-y^2 \rightarrow xz, yz$ )
	$^2A$	30811	28% CTLM ( $14a \rightarrow x^2-y^2$ ), 63% LF ( $x^2-y^2 \rightarrow z^2$ )
	$^2A$	34233	64% CTLM ( $14a \rightarrow x^2-y^2$ ), 28% LF ( $x^2-y^2 \rightarrow z^2$ )
	$^2A$	36966	95% CTLM ( $13a \rightarrow x^2-y^2$ )
	$^2B_1$	33877	93% CTLM ( $15b_1 \rightarrow x^2-y^2$ )
	$^2B_1$	39909	96% CTLM ( $14b_1 \rightarrow x^2-y^2$ )

<sup>a</sup> CASPT2 excitation energies based on state average CASSCF (no counterions) for different active spaces. These preliminary results indicate that the ground state of the dodecahedral complex is  $^2A$  ( $^2B_1$  in  $D_{2d}$ ) ( $d_{x^2-y^2}$ )<sup>1</sup> and that the lowest excitations are CTLM. For the 17i13 active space no convergence could be achieved in the case of the  $^2B_2$  states.

electronic structure in the sense that the second low-lying CTLM originating from a lower lying ligand level was found. Due to the limitations of the active space this transition could not be calculated with the (9i13) active space. An analysis of the CASSCF results revealed that the contributions to the wave function are mainly due to exchanges of an electron among levels that belong to the same irrep. On the basis this experience it is clear that the only possible way to calculate all states relevant to the electronic spectrum, while at the same time incorporating all the near-degeneracy effects, is to use four different active spaces, one for each irrep of  $D_2$ . Common to the four different active spaces are the five  $d$  orbitals. For each irrep these orbitals are supplemented by all  $5\sigma$  and  $1\pi$  levels of that particular symmetry (six in total for each symmetry) giving rise to four (13i11) active spaces. In this way all the  $d-d$  transitions and all the low-lying CTLM transitions are accessible. Doublet spin states are calculated at the CASPT2 level using the molecular orbitals that are obtained from average CASSCF calculations that included 8 states for the  $^2A$  symmetry and 7 states for the other three symmetries. The excitation energies for the states belonging to a particular symmetry were derived by calculating the ground state with the active space of that symmetry. In this way we can have an idea about the performance of the computational model used. It was found that the energies of the ground state changed for no more than  $1200\text{ cm}^{-1}$  between the various active spaces, a value that allows us to make reliable predictions about the nature of the transitions in the experimental spectrum. Previous CASPT2 calculations on  $\text{Cr}(\text{CO})_6$  have successfully employed the same strategy for calculating the electronic spectrum.<sup>17</sup>

Using this computational scheme the influence of the Madelung potential on excitation energies was studied. Figure 2 depicts the effect of the crystal surroundings. Most transitions are shifted downward when counterions are

(16) Vanquickenborne, L. G.; Hendrickx, M.; Hyla-Krispin, I.; Haspeslagh, L. *Inorg. Chem.* **1986**, *25*, 885.

(17) Pierloot, K.; Tsokos, E.; Vanquickenborne, L. G. *J. Phys. Chem.* **1996**, *100*, 16545.



**Table 2.** CASPT2 Excitation Energies Obtained for the Dodecahedral Isomer by Using the Molecular Orbitals of State Average CASSCF (13i11) Calculations, Including the Madelung Potential<sup>a</sup>

excited state	excitation energy (cm <sup>-1</sup> )	nature of transition	oscillator strength	exptl <sup>b</sup> (cm <sup>-1</sup> )
<sup>2</sup> A	25311	52% CTLM (13a→x <sup>2</sup> -y <sup>2</sup> ), 35% LF (x <sup>2</sup> -y <sup>2</sup> →z <sup>2</sup> )		
	31041	35% CTLM (13a→x <sup>2</sup> -y <sup>2</sup> ), 61% LF (x <sup>2</sup> -y <sup>2</sup> →z <sup>2</sup> )		
	34919	98% CTLM (14a→x <sup>2</sup> -y <sup>2</sup> )		
	35461	88% CTLM (12a→x <sup>2</sup> -y <sup>2</sup> )		
	46727	83% CTLM (11a→x <sup>2</sup> -y <sup>2</sup> ),		
	48676	79% CTLM (13a→z <sup>2</sup> )		
	53789	73% CTLM (14a→z <sup>2</sup> )		
<sup>2</sup> B <sub>1</sub>	28061	98% CTLM (15b <sub>1</sub> →x <sup>2</sup> -y <sup>2</sup> )	0.000000	
	33815	98% CTLM (14b <sub>1</sub> →x <sup>2</sup> -y <sup>2</sup> )	0.002405	
	37204	95% CTLM (13b <sub>1</sub> →x <sup>2</sup> -y <sup>2</sup> )	0.000001	
	37972	96% CTLM (11b <sub>1</sub> →x <sup>2</sup> -y <sup>2</sup> )	0.000000	
	41114	98% CTLM (12b <sub>1</sub> →x <sup>2</sup> -y <sup>2</sup> )	0.064714	39800 (?)
	43474	93% CTLM (10b <sub>1</sub> →x <sup>2</sup> -y <sup>2</sup> )	0.000000	
	47698	97% LF (x <sup>2</sup> -y <sup>2</sup> →xy)	0.000000	
<sup>2</sup> B <sub>2</sub>	26025	91% CTLM (15b <sub>2</sub> →x <sup>2</sup> -y <sup>2</sup> )	0.021892	25800
	31386	92% CTLM (14b <sub>2</sub> →x <sup>2</sup> -y <sup>2</sup> )	0.000126	
	30955	91% CTLM (13b <sub>2</sub> →x <sup>2</sup> -y <sup>2</sup> )	0.015344	32000
	36634	85% CTLM (12b <sub>2</sub> →x <sup>2</sup> -y <sup>2</sup> )	0.039816	36800, 39800 (?)
	38589	97% CTLM (11b <sub>2</sub> →x <sup>2</sup> -y <sup>2</sup> )	0.010918	36800, 39800 (?)
	44667	90% LF (x <sup>2</sup> -y <sup>2</sup> →xz)	0.003208	
	44713	95% CTLM (15b <sub>2</sub> →z <sup>2</sup> )	0.000167	
<sup>2</sup> B <sub>3</sub>	26202	96% CTLM (15b <sub>3</sub> →x <sup>2</sup> -y <sup>2</sup> )	0.021075	25800
	30850	97% CTLM (14b <sub>3</sub> →x <sup>2</sup> -y <sup>2</sup> )	0.000001	
	31398	88% CTLM (13b <sub>3</sub> →x <sup>2</sup> -y <sup>2</sup> )	0.014880	32000
	36317	86% CTLM (12b <sub>3</sub> →x <sup>2</sup> -y <sup>2</sup> )	0.035315	36800, 39800 (?)
	38418	96% CTLM (11b <sub>3</sub> →x <sup>2</sup> -y <sup>2</sup> )	0.007400	36800, 39800 (?)
	44085	93% LF (x <sup>2</sup> -y <sup>2</sup> →yz)	0.002850	
	45984	94% CTLM (10b <sub>3</sub> →x <sup>2</sup> -y <sup>2</sup> )	0.000008	

<sup>a</sup> States and orbitals labeled according to the  $D_2$  point group. Comparison with the experimental spectrum of  $\text{Mo}(\text{CN})_8^{3-}$  in aqueous solution. <sup>b</sup> Reference 6.

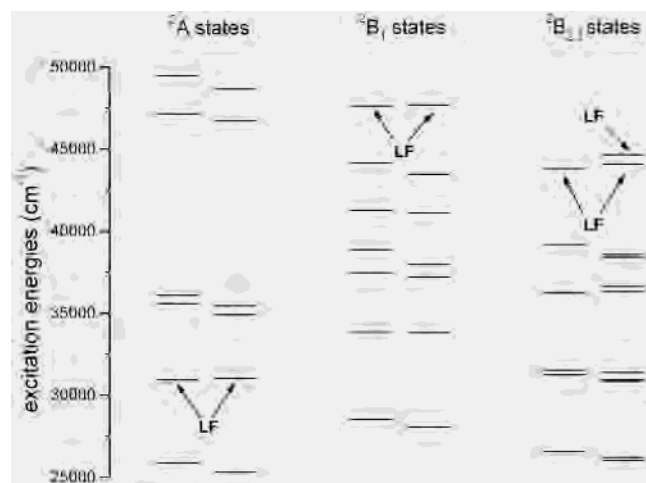


**Figure 2.** Influence of the Madelung potential on the CASPT2 excitation energies for the dodecahedral structure. For each symmetry the right and the left column represent the excitation energies with and without point charges, respectively. LF indicates ligand field (d-d) transitions.

incorporated in the calculation. The extent, however, is limited, on the average amounting to about 500 cm<sup>-1</sup>. This implies that the Madelung potential in the region of the  $\text{Mo}(\text{CN})_8^{3-}$  complex is rather flat. Without any doubt the observed shifts do not exceed the accuracy of our calculations. The splitting of the <sup>2</sup>E ( $D_{2d}$ ) states in <sup>2</sup>B<sub>1,2</sub> at the far right-hand side of Figure 2 is even less, reflecting the fact the  $D_{2d}$  symmetry is to a large extent conserved. This allows us to classify the various states of the complex according to this point group. For the discussion of the electronic structure

of the  $\text{Mo}(\text{CN})_8^{3-}$  complex and the comparison with the experimental spectrum in the following paragraphs we have chosen to use the results of the CASSCF and CASPT2 calculations that incorporate the Madelung potential. Although we feel that incorporating the crystal surroundings makes the computational model more realistic, it is, however, not essential for obtaining a qualitative and even quantitative description of the electronic properties of  $\text{Mo}(\text{CN})_8^{3-}$ . This conclusion was also obtained for the hexacyano complexes of the first-row transition metal cations, where it was found that CASPT2 calculations without incorporating the counterions were able to reproduce the experimental spectra either for aqueous solutions or for solids.<sup>11</sup>

The experimental spectrum exhibits four distinct absorption bands in the region between 25000 and 40000 wavenumbers. The lower energy part shows two intense absorptions at 25800 and 32000 cm<sup>-1</sup>, possessing extinction coefficients of 1350 and 800 at their maxima, respectively. Two nearly equal and even more intense bands are observed at 36800 ( $\epsilon = 2000$ ) and 39800 cm<sup>-1</sup> ( $\epsilon = 1900$ ). Comparing these experimental values with our calculated CASPT2 energies in Table 2 shows that an unambiguous assignment based solely on excitation energies is not possible. A close inspection of Table 2 shows that between 25000 and 42000 cm<sup>-1</sup> no fewer than 14 states can possibly be at the origin of the observed absorption bands. Additional information is therefore needed. For this purpose the oscillator strengths for the transitions from the ground state to all the <sup>2</sup>B<sub>1</sub>, <sup>2</sup>B<sub>2</sub>, and <sup>2</sup>B<sub>3</sub> states are calculated by using the CASSCF wave

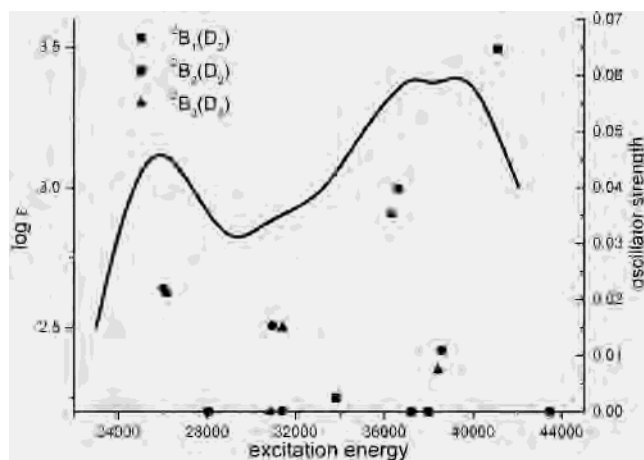


**Figure 3.** Comparison of the theoretical results for the dodecahedral geometry (CASSCF oscillator strengths versus CASPT2 excitation energies) with the experimental spectrum ( $\log \epsilon$  versus wavenumbers) in aqueous solution.<sup>6</sup>

functions. Transitions to  ${}^2A$  states need not be considered because they are symmetry-forbidden.

The obtained oscillator strengths are collected in Table 2 and represented graphically in Figure 3. A first remarkable conclusion concerns the d–d transitions. Compared to the CTLM transitions all of them are less intense and are therefore not observable in the experimental spectrum. The reason for their low intensity is the high oxidation state of the molybdenum cation that does not allow extensive covalent mixing with the ligand orbitals to occur, implying that the selection rules for the pure d orbitals hold rather strongly for these transitions. For the  ${}^2B_1$  group of states only two CTLM transitions give rise to more or less intense absorption bands: a somewhat less intense transition at  $33815\text{ cm}^{-1}$  and a far more intense one at  $41114\text{ cm}^{-1}$ . Inspection of the orbitals shows that these excitations involve levels which transform almost as an  $a_2$  irrep of the  $D_{2d}$  point group, resulting in excitations  $1,2a_2 (D_{2d}) \rightarrow d_{x^2-y^2} (b_1 \text{ in } D_{2d})$ , which are dipole allowed. For the other transitions in the  ${}^2B_1$  group of states an electron is transferred from a  $b_2 (D_{2d})$  like orbital to  $d_{x^2-y^2}$ . Our calculated oscillator strengths in  $D_2$  indeed confirm that these excitations are to a very large extent forbidden. Again we can conclude that although the incorporation of counterions in our model reduces formally the symmetry to  $D_2$ , the effective symmetry of the electronic structure of the  $\text{Mo}(\text{CN})_8^{3-}$  part remains largely  $D_{2d}$ .

Within the  ${}^2B_2$  and  ${}^2B_3$  group ( ${}^2E$  in  $D_{2d}$ ) transitions in general are more intense, reflecting that these transitions are symmetry allowed. A comparison with the experimental spectrum in Figure 3 shows a rather good correspondence for the low-energy part. Transitions at  $25800$  and  $32000\text{ cm}^{-1}$  can be ascribed to excitations from two shells:  $15b_2, b_3$  and  $13b_2, b_3$ , respectively. For the high-energy part of the spectrum our calculations are not conclusive. It is possible that the band at  $36800\text{ cm}^{-1}$  is due to excitations from the two close-lying  $11b_2, b_3$  and  $12b_2, b_3$  shells, in which case the highest energy band in the spectrum corresponds to an excitation to the  ${}^2B_1$  state. However, the fact that the two absorptions at  $36800$  and  $39800\text{ cm}^{-1}$  are almost equally intense points rather to a split  ${}^2B_{2,3}$  state (distortion of the

dodecahedral  $\text{Mo}(\text{CN})_8^{3-}$  structure), implying that the  ${}^2B_1$  transition is calculated too low by the CASPT2 method. Whatever may be the case, we can safely state that all excitations observable in the experimental spectrum are of the CTLM type and involve transitions of an electron from ligand orbitals to  $d_{x^2-y^2}$  of molybdenum.

The important metal valence d orbitals and the nature of the ligand orbitals that are involved in the experimentally observed spectrum are depicted in Figures 4 and 5, respectively. These figures show the natural orbitals that are nearly singly occupied in the root (average state CASSCF calculation) corresponding to a specific ligand field or charge transfer state. Figure 4a shows the 15a orbital which is almost a pure  $d_{x^2-y^2}$  metal orbital. The minute ligand part of this orbital is mainly located on the equatorial cyanides, the axial ligands contributing much less. The explanation for this observation can be found in the larger overlap of  $d_{x^2-y^2}$  with the orbitals of the equatorial ligands. The character of the covalent mixing can be seen to be completely of  $\pi$  type. Plots b–e of Figure 4 show the 16a, 16b<sub>1</sub>, 16b<sub>2</sub>, and 16b<sub>3</sub> metal orbitals which are predominantly of  $d_z^2$ ,  $d_{xy}$ ,  $d_{xz}$ , and  $d_{yz}$  character, respectively. Contrary to the 15a orbital ( $d_{x^2-y^2}$ ) the main ligand contribution to these orbitals is of the  $5\sigma$  type with only a small contribution of the  $1\pi$  orbitals, the overall covalent mixing being much more pronounced. A common feature of all the metal type orbitals, including  $d_{x^2-y^2}$ , is their antibonding nature with respect to the ligand orbitals. This places them energetically above the occupied  $1\pi$  and  $5\sigma$  orbitals of the cyanide ligands. Hence, the calculated ligand field splitting of the 4d shell on Mo (Table 2) can nicely be rationalized by simple angular overlap model (AOM) considerations. According to AOM the transition energies in an idealized  $ML_8$  dodecahedron as a function of the ligand  $e_\sigma$  and  $e_\pi$  parameters are given by

$$E(x^2-y^2 \rightarrow z^2) = 1.243 e_\sigma - 0.894 e_\pi$$

$$E(x^2-y^2 \rightarrow xz, yz) = 2.029 e_\sigma - 2.133 e_\pi$$

$$E(x^2-y^2 \rightarrow xy) = 2.699 e_\sigma - 3.599 e_\pi$$

Using an average  $e_\sigma$  parameter of  $33000\text{ cm}^{-1}$  and a ratio of  $e_\sigma/e_\pi = 3$ , transitions are predicted at  $31185$ ,  $43494$ , and  $49478\text{ cm}^{-1}$ , in good agreement with the corresponding values of  $31041$ ,  $44376$ , and  $47698\text{ cm}^{-1}$  in the present calculations.

The ligand orbitals giving rise to large absorptions, i.e.,  $12b_1$ ,  $11b_2$ ,  $12b_2$ ,  $13b_2$ , and  $15b_2$ , are represented in plots a–e of Figure 5. All these orbitals have metal contributions that are small, demonstrating that the bonding in the complex is to a large extent ionic. Covalent effects can be observed and are more pronounced in ligand orbitals that are predominantly  $5\sigma$ , as for instance in  $12b_2$ , which has a small but noticeable contribution of  $d_{xz}$ . Although for the uncoordinated cyanide the  $5\sigma$  orbital is positioned above the  $1\pi$  orbital, the stronger  $\sigma$  bonding interactions in the complex stabilize the former orbitals more. The  $5\sigma$  orbitals are now

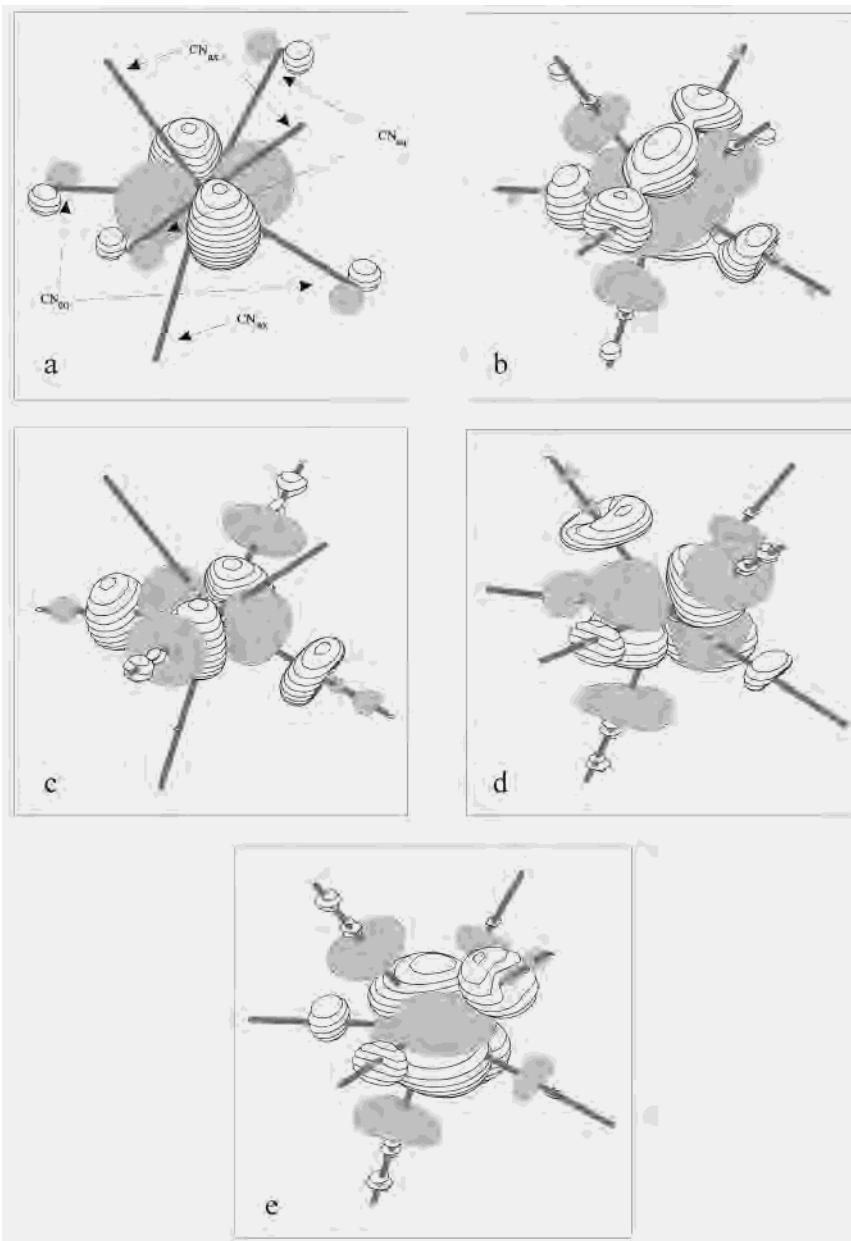


**Figure 4.** Three-dimensional plots of the CASSCF natural orbitals. Figures show orbitals of the dodecahedral isomer with predominant molybdenum d character: (a)  $d_{x^2-y^2}$ , (b)  $d_{z^2}$ , (c)  $d_{xy}$ , (d)  $d_{xz}$ , and (e)  $d_{yz}$ . Surfaces drawn for orbital function values of  $\pm 0.05(\text{\AA})^{-3/2}$ .

situated either among the  $1\pi$  orbitals as demonstrated by the  $12b_2$  or even below the  $1\pi$  orbitals as illustrated by the low-lying  $10b_3$  in Figure 5f.

Although our calculations on the dodecahedral structure of  $\text{Mo}(\text{CN})_8^{3-}$  explain rather nicely the experimental spectrum as recorded for an aqueous solution, we started calculations for the *square-antiprism* structure. In this way we will be able to further substantiate our statement about the nature of the structure that is responsible for the observed electronic transitions. Because no experimental X-ray data are available for this isomer of the octacyanomolybdate(V) anion, the bond distance of the dodecahedral structure was taken, while the angle between the Mo–C internuclear axis and the  $S_8$  axis was set equal to  $58.0^\circ$ , which is an average value of the experimental angles found in the square-antiprism geometries of  $\text{W}(\text{CN})_8^{3-}$ .<sup>18,19</sup> The level of

sophistication of the computations (basis sets, method, and strategy) is the same as the one used for the dodecahedral geometry, so that the two sets of data can be compared. A perfect  $D_{4d}$  geometry for the  $\text{Mo}(\text{CN})_8^{3-}$  anion was imposed. As can be anticipated from simple ligand field calculations,<sup>6</sup> the CASPT2 method predicts a  ${}^2A_1$  ground state with the unpaired valence electron occupying the  $d_{z^2}$  orbital. The ligand field transition to the  $e_2$  ( $d_{xy}$ ,  $d_{x^2-y^2}$ ) shell is situated at  $38970\text{ cm}^{-1}$ , and the excitation to the  $e_3$  ( $d_{xz}$ ,  $d_{yz}$ ) shell can be expected at  $47920\text{ cm}^{-1}$ . In parallel with the results for the dodecahedral isomer the charge transfer transitions of the type ligand to metal are calculated to be the lowest lying excited states for the square antiprism. These types of

(18) Bok, L. C. D.; Leipoldt, J. G.; Basson, S. S. *Acta Crystallogr.* **1970**, B26, 684.

(19) Basson, S. S.; Bok, L. D.; Leipoldt, J. G. **1970**, B26, 1209.

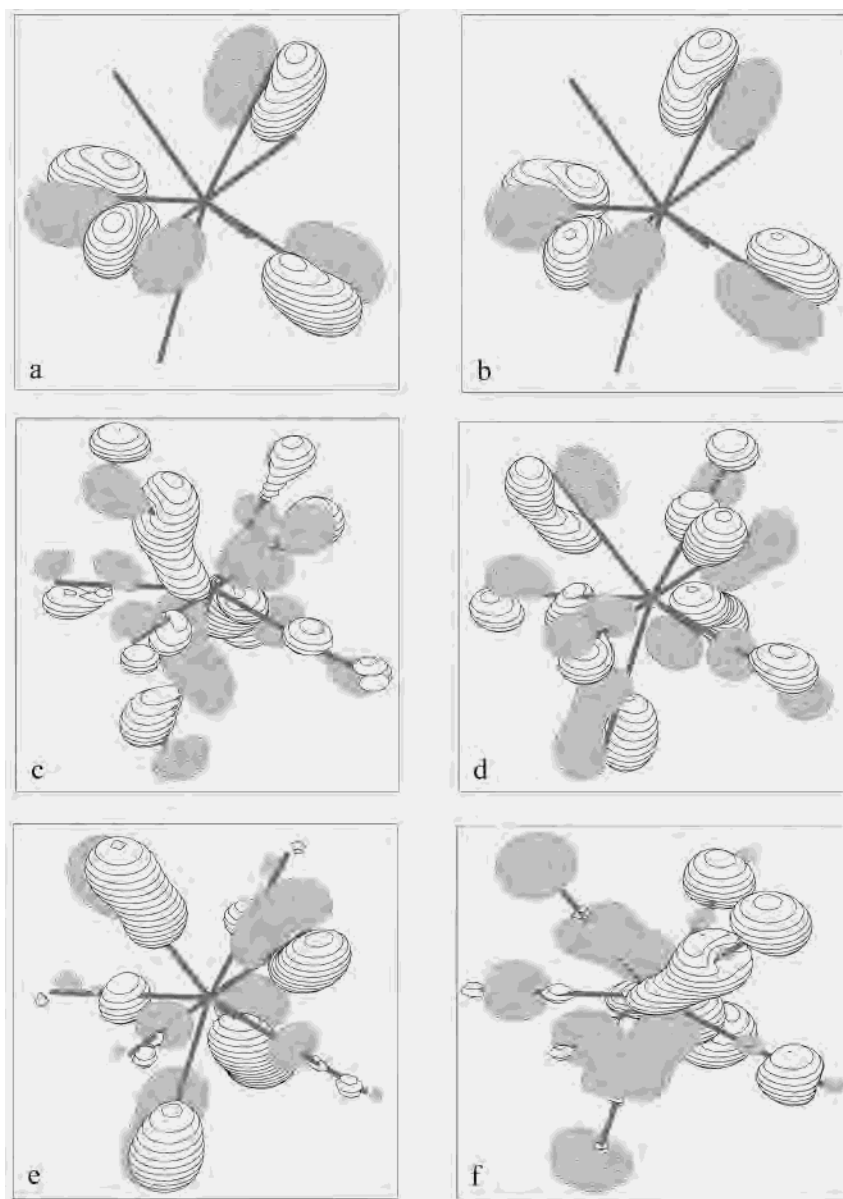


**Figure 5.** Three-dimensional plots of the CASSCF natural orbitals. Figures show orbitals of the dodecahedral isomer with predominant cyanide character: (a)  $12b_1$ , (b)  $11b_2$ , (c)  $12b_2$ , (d)  $13b_2$ , (e)  $15b_2$ , and (f)  $10b_3$ . Surfaces drawn for orbital function values of  $\pm 0.05(\text{\AA})^{-3/2}$ . The  $\text{Mo}(\text{CN})_8^{3-}$  complex is placed in the same position as in Figure 4.

states are spread out more or less evenly between  $25000$  and  $50000\text{ cm}^{-1}$ . However, calculated oscillator strengths reveal that only two transitions are predicted to have large intensities, while the other charge-transfer transitions and ligand field excitations possess intensities that are more than 10 times less. Of the two transitions with high intensities the lowest is positioned at  $24996\text{ cm}^{-1}$  and corresponds to an excited state of  ${}^2B_2$  symmetry, while the highest transition involves a  ${}^2E_1$  state that lies  $37794\text{ cm}^{-1}$  above the ground state. In between these two transitions our theoretical treatment of the square-antiprism structure predicts a spectroscopic window with no intense transitions. In the experimental spectrum (Figure 3) a transition is observed at  $32000\text{ cm}^{-1}$ , so that we are inclined to reject this isomer of  $\text{Mo}(\text{CN})_8^{3-}$  as being responsible for the experimental spectrum of this complex in aqueous solution. Our calculations suggest its structure to be dodecahedral.

## Conclusion

The calculated CASPT2 transition energies and associated oscillator strengths indicate that the dodecahedral structure is likely to be responsible for the absorption spectrum of  $\text{Mo}(\text{CN})_8^{3-}$ , not the square antiprism as advocated by Golebiewski et al. All observed transitions are of the CTLM type, contrary to the proposition of Perumareddi et al., who claimed d–d transitions to be responsible. The Madelung potential is quite flat so that the crystal surroundings do not influence the excitation energies. Both metal basis sets used are able to reproduce the experimental spectrum. From the magnetic point of view, especially the nature of the semi-occupied  $d_{x^2-y^2}$  and the other unoccupied d orbitals is of importance. The magnetic orbital  $d_{x^2-y^2}$  shows admixture with the  $\pi$  orbitals of the ligands only while all other d orbitals are hybridized with  $5\sigma$  orbitals of cyanide. One can observe

that  $\sigma$  covalency in these orbitals is much stronger than the  $\pi$  interactions. This gives direct support to our previous hypothesis that the observed ferromagnetism in the Mo<sup>V</sup>–CN–Mn<sup>II</sup> dimer is strongly promoted via a  $\sigma$  channel between the magnetic orbitals of the manganese and the virtual d orbitals of the molybdenum. The calculations also convincingly demonstrate that  $d_{x^2-y^2}$  is almost an ideal example of a  $\sigma$  nonbonding orbital. Antiferromagnetic interaction in the ground state thus can only take place via

a weaker  $\pi$  channel, again in agreement with the previous hypothesis.

**Acknowledgment.** Financial support by the Belgian National Science Foundation and the Flemish Government under the Concerted Action Scheme are gratefully acknowledged. We thank V. Mironov for a discussion of the ligands field results.

IC0258734